Journal Pre-proof

Preparation and combustion properties of laminated sticks of B–CuO and B–Bi_2O_3

Song Haoyu, Li Chenyang, Gao Fubing, Chongwei An, Li Shijiao, Zhan Xuan, He Jianchen

PII: S2214-9147(24)00012-6

DOI: https://doi.org/10.1016/j.dt.2024.01.002

Reference: DT 1388

To appear in: *Defence Technology*

Received Date: 23 September 2023

Revised Date: 30 December 2023

Accepted Date: 15 January 2024

Please cite this article as: Haoyu S, Chenyang L, Fubing G, An C, Shijiao L, Xuan Z, Jianchen H, Preparation and combustion properties of laminated sticks of B–CuO and B–Bi_2O_3, *Defence Technology* (2024), doi: https://doi.org/10.1016/j.dt.2024.01.002.

Preparation and combustion properties of laminated sticks of B-CuO and B-Bi_2O_3

Haoyu Song [a], Chenyang Li [a], Fubing Gao [a], Chongwei An [a,*], Shijiao Li [a], Xuan Zhan [a], Jianchen He [b]

[a] School of Environment and Safety Engineering, North University of China, Taiyuan 030051, China

[b] Chongqing Military Agency of the Army, Chongqing 400060, China

***Corresponding author:** Chongwei An
E-mail: anchongwei@yeah.net

Preparation and combustion properties of laminated sticks of B-CuO and B-Bi_2O_3

Abstract

To explore the composite process of B-CuO and B-Bi_2O_3 two-component laminated sticks, obtain the corresponding sticks with good printing effect, and explore the energy release behavior. In this study, boron, copper oxide, and bismuth trioxide powders were dispersed in the dispersed phase (DMF) using F_{2602} as a binder, and the construction of two-component B-CuO, B-Bi_2O_3, three-component micro-composite, and three-component macro-composite sticks were realized with the help of double nozzle direct ink writing (DIW) technique respectively. The resulting sticks were ignited by a nichrome wire energized with a direct current, and a high-speed camera system was used to record the combustion behavior of the sticks, mark the flame position, and calculate the rate of ignition. The results showed that the B-CuO stick burning rate (42.11 mm·s^{-1}) was much higher than that of B-Bi_2O_3 (17.84 mm·s^{-1}). The formulation with the highest CuO content (ω_{CuO}=58.7%) in the microscale composite of the sticks also had the fastest burning rate of 60.59 mm·s^{-1}, as the CuO content decreased (ω_{CuO}=43.5%, 29.3%), its burning rate decreased to 34.78 mm·s^{-1}, 37.97 mm·s^{-1}. The stick with the highest copper oxide content (ω_{CuO}=60%) also possessed the highest burning rate (48.84 mm·s^{-1}) in the macro-composite sticks, and the burning rates of the macro-composite sticks with component spacing of 0.1 mm, 0.2 mm, and 0.5 mm were 43.34 mm·s^{-1}, 48.84 mm·s^{-1}, and 40.76 mm·s^{-1}.

Keywords: Boron-based thermite; Direct ink writing; Linear burning rate; Multi-component composite

1. Introduction

As a typical class of composite energy-containing materials, thermite, which consists of fuel, oxidizer, and additives [1–4], due to its characteristics of intense redox reaction and release of large amounts of heat under the stimulation of external energy, is widely used in material synthesis [5], thermal welding [6], thermal cutting [7], micro-propulsion [8], etc. Among many fuels, boron has been regarded as a very promising fuel due to its high mass calorific value and volumetric calorific value [9]. However, boron itself is easy to oxidize and difficult to ignite, and other defects limit its wide application [10]. To overcome the combustion shortcomings of boron-based thermite and improve its combustion efficiency, scholars have carried out a lot of research, which shows that the addition of metal oxides can reduce the combustion reaction temperature of boron [11–13], thus improving the characteristics of boron difficult to ignite. Among many metal oxides, CuO and Bi_2O_3 are proven to be the most effective substances for boron ignition and combustion [14], and the synergistic enhancement effect produced by the multicomponent composite powders of these two metal oxides [14] reduces their chemical onset reaction temperature [15], resulting in a better ignition effect and higher energy release rate.

It is worth noting that the vast majority of scholarly research on boron-based thermite focuses on the improvement of powder material proportioning and composite modification on the thermal behavior of the powder. Therefore, it is necessary to carry out powder integration of B-CuO and B-Bi_2O_3 powders and study the effect of different integration methods on their combustion performance. As a rapidly emerging and mature technology in recent years, additive manufacturing technology provides a platform for low-cost, multi-scale, and high degree-of-freedom molding of composite powders [16, 17]. At present, many scholars have carried out some exploration and application in the direction of igniter [18, 19], delay composition [20], thermite [21, 22], booster explosive [23, 24], etc., and obtained the performance of a single formula under the excellent samples. With the molding and development of direct ink writing technology, multi-component, complex morphology of stick manufacturing has become possible. At present, there are scholars with the help of DIW technology to obtain the hollow linear structure [25] and gradient loading structure [26]. In summary, with the help of the double nozzle direct ink writing technique for three-component ink structure accumulation, achieving multi-scale, diverse stick preparation has a certain degree of feasibility, the application of this technology will also provide more possibilities for the composite of multi-component powder materials.

In order to realize the integration and construction of multi-component powders, explore diverse powder compounding methods. It is proposed to use F_{2602} to disperse B, CuO, and B, Bi_2O_3 in DMF, and obtain two-component B-CuO ink and B-Bi_2O_3 ink by centrifugal mixer, and then based on this two-component ink, the above ink is mixed and extruded in different ratios to produce microscopic scale composite sticks. With the help of a double nozzle direct ink writing device, the three-component ink was accumulated layer by layer with different thicknesses to produce macro-composite sticks. The flame behavior was captured by high-speed photography, the burning rate was calculated, and the crystal shape of the combustion products was tested, thus condensing the energy release law of the microscopic and macroscopic composite of the stick. This study not only provides a new method of direct writing with double nozzle direct ink writing for the micro-size integration and assembly of B, CuO, and Bi_2O_3 powders, but also the experimental data obtained provide new ideas for the reactivity modulation and functionalization of B, CuO, and Bi_2O_3, and also enrich the study of the energy release behaviors of boron-based thermite.

2. Experimental section

2.1. Materials

CuO and Bi_2O_3 were purchased from Nangong Bole Metal Materials Co., Ltd.; Amorphous boron was purchased from Hebei Flance Nanotechnology Co., Ltd; F_{2602} was purchased from Chenguang Research Institute of Chemical Industry; N, N-Dimethylformamide was purchased from Shanghai Macklin Biochemical Technology Co., Ltd.

2.2. Preparation and direct writing of B-CuO and B-Bi_2O_3 inks

F_{2602} with a mass fraction of 5% was homogeneously dispersed in a certain amount of DMF under mechanical stirring, after which amorphous B, CuO, and Bi_2O_3 of $1^{\#}$ and $2^{\#}$ in Table 1 were added, and the powders were mixed in a centrifugal mixer at 1200 rpm for 60 s, so that each powder could be homogeneously dispersed in a binder system, and B-CuO, B-Bi_2O_3 inks were produced. In order to make the stick combustion effect is the best, taking into account the slow oxidation of boron in the air and other factors, we choose the equivalent ratio of 1.5.

Table 1

Ink formulations for DIW systems.

Sample	Mass ratio			F_{2602}	remark
	B	CuO	Bi_2O_3		
$1^{\#}$	12.0	88.0	-	5	Φ=1.5
$2^{\#}$	6.5	-	93.5	5	Φ=1.5
$3^{\#}$	10.2	58.7	31.1	5	$1^{\#}$:$2^{\#}$=2:1
$4^{\#}$	9.3	43.5	47.2	5	$1^{\#}$:$2^{\#}$=1:1
$5^{\#}$	8.3	29.3	62.4	5	$1^{\#}$:$2^{\#}$=1:2

The direct ink writing method of two-component ink is as follows, the direct writing syringe filled with ink is fixed on the direct writing platform, and the temperature of the platform is set to 40 °C to ensure the rapid molding of the ink and provide certain support effects for the next layer of ink. Select the inner diameter of 0.65 mm direct writing needle, needle from the initial height of the substrate 0.2 mm, layer height setting 0.1 mm, programmed in the controller, so that the needle achieves accurate movement on the *X*, *Y*, and *Z* axis. The direct writing needle accumulates ink layer by layer on the plexiglass substrate at a travel speed of 4.5 mm·s^{-1} and an extrusion speed of 1 mm·s^{-1}.

The micro-scale composite of the three-component ink is centrifugal mixing of two-component B-CuO and B-Bi_2O_3 inks at mass ratios of 2:1, 1:1, 1:2, from which ink samples of No. 3#, No. 4#, and No. 5# (Table 1, Fig. 1) are made, in which CuO and Bi_2O_3 are homogeneously mixed on the microscopic scale. With the help of the DIW system can be obtained layer by layer-by-layer accumulation of microscopic scale composite sticks.

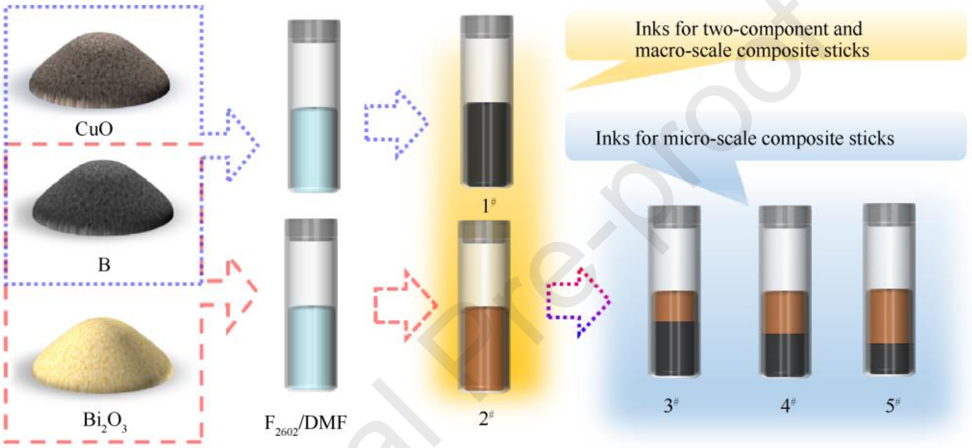

Fig. 1. Configuration of B-CuO, B-Bi_2O_3 two-component and micro-scale composite inks.

Macro-scale of three-component inks can be achieved with the help of a double nozzle direct ink writing device (Fig. 2(a)). Nozzle 1 and Nozzle 2 were filled with two-component 1# and 2# inks, and the two nozzle switching methods were adjusted in an orderly manner through the controller, thus obtaining macroscopic-scale composite sticks with a component spacing of 0.1 mm (sample referred to as BCBC, letter B refers to component 2#, letter C refers to component 1#), 0.2 mm (sample referred to as BBCC), and 0.5 mm (sample referred to as 5B5C). The prepared sticks were dried in an oven at 55 °C for 72 h to evaporate the solvent DMF.

2.3. SEM, EDS, XRD tests

The molding effect of the sticks was characterized by an LSM-900 laser scanning microscope. The microscopic morphology of Boron/Metal oxide sticks was investigated by scanning electron microscopy (SEM), and the distribution of the components in the sticks was characterized by energy dispersive spectroscopy (EDS) under different formulations. The crystal composition of the combustion solid products was tested using a DX-2700 X-ray diffractometer (XRD).

2.4. DSC-TG tests

We performed DSC-TG tests on B-CuO and B-Bi_2O_3 sticks (with an equivalence ratio of 1.5) using Netzsch STA 449 F3.

2.5. Combustion Behavior Test

A length of 30 mm stick was intercepted and fixed on a glass plate, and the stick was ignited by a high-heat nichrome wire with a 32 V DC power supply. The combustion process of the sticks was recorded by i-SPEED 221 high-speed cameras (iX Cameras), which captured the macroscopic combustion effect of the stick at a frame rate of 2000 fps and an exposure time of 300 μs, and the microscale combustion effect of the stick at a frame rate of 1000 fps and an exposure time of 100 μs. The burning speed of the sticks was calculated from the X-direction displacement of the burning flame of the sticks per unit of time.

3. Result and discussion

3.1. Macroscopic and microscopic elemental distribution of sticks

We used only a 5% mass fraction of F_{2602} as a binder and loaded B, CuO, and Bi_2O_3 into the dispersed-phase DMF via a centrifugal mixer to form energy-containing inks of the corresponding formulation. The viscosity of this ink decreases sharply when the shear rate is increased, and then stabilizes with a shear-thinning property, which allows the ink to be smoothly deposited on the substrate by the direct writing needle when pushed by the gas. Under the thermal action of the platform, the DMF on the surface of the ink undergoes a small amount of volatilization, forming a skeleton containing fuel, oxidizer, and binder, which provides some support for the direct writing of the next layer of ink, which accumulates layer by layer, realizing the powder integration of boron and oxidizer.

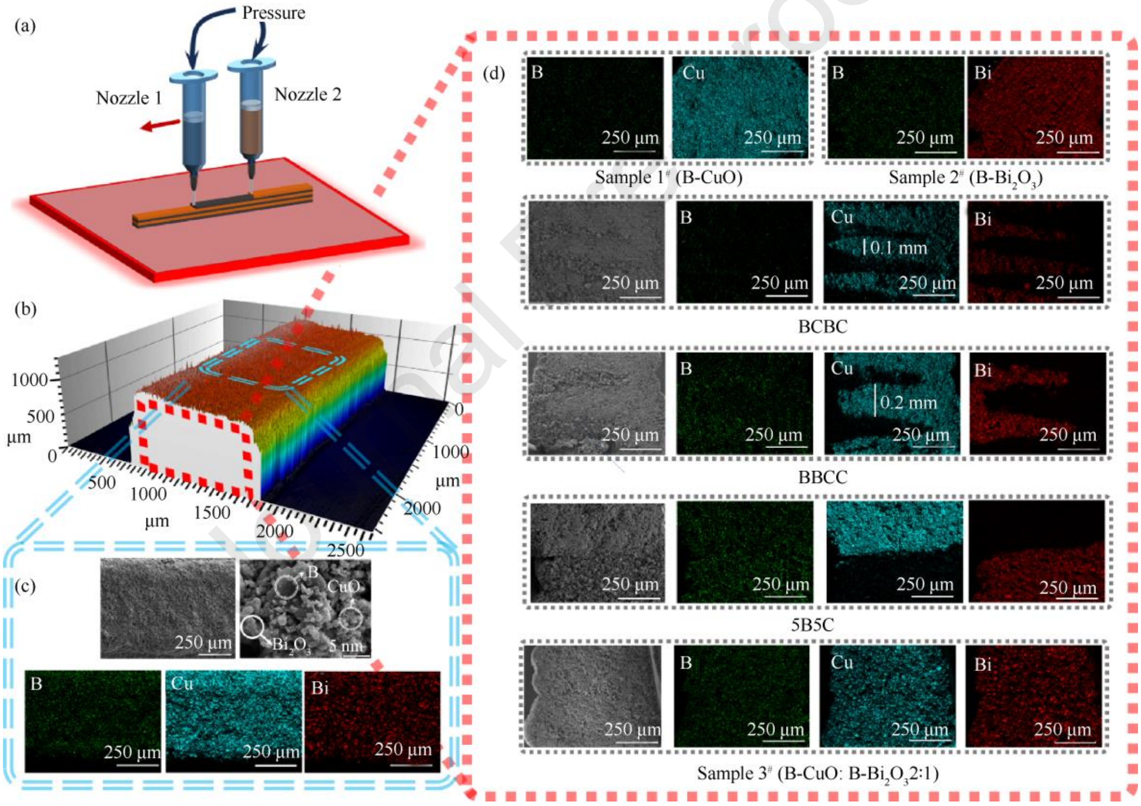

Fig. 2. (a) Working schematic of the double nozzle direct ink writing stick; (b) Macroscopic scan of the stick; (c) Microscopic scan of the surface of formulation 3# stick; (d) Microscopic scan of the cross-section of the sticks.

Fig. 2(b) shows the 3D scanning image of the B-CuO-Bi_2O_3 stick (BCBC) fabricated by the double-jet direct-write technique, which has a cross-section of about 1 mm×1 mm with a good rectangularity. The connection between the layers of the stick is tight, without delamination, fracture, and other phenomena, showing a good molding effect. The EDS tests on the surface and cross-section of the sticks (Figs. 2(c) and 2(d)) show that the two-component B-CuO and B-Bi_2O_3 inks are uniformly dispersed after centrifugal mixing of the powders, forming a stable ink system without particle settling or delamination. The micrometer scale is a homogeneous dispersion of oxidant nanoparticles near amorphous boron, which makes it easier for the fuel and oxidant to come into contact with the stick when it is heated and thus reacts vigorously. In addition, the highly homogeneous mixing of the particles will also improve the combustion stability and burning rate error of the stick.

The three-component ink's double nozzle direct ink writing stick reflects a good particle distribution effect, the B-CuO part and the B-Bi_2O_3 part are accumulated layer by layer with a preset program, and the ink is stable in the process of direct writing and deposition, and there is no migration of particles in different inks. The presence of a clear elemental demarcation line in the cross-section of the stick demonstrates that the double nozzle direct ink writing technology enables precise layer-by-layer accumulation of multi-component inks.

3.2. Combustion of two-component sticks

To study the combustion performance of the macro-scale and micro-scale composite of B-CuO and B-Bi_2O_3 sticks, the macroscopic and microscopic combustion behaviors of the two-component sticks of B-CuO and B-Bi_2O_3 should first be investigated. Figs. 3(a) and 3(b) show the snapshots of the combustion process of B-Bi_2O_3 and B-CuO with an equivalence ratio of 1.5, respectively. The uniform distribution of the components of the stick produced with the help of DIW technology makes the stick stable in the mass and heat transfer process during combustion, and a similar flame combustion phenomenon is observed at all time nodes. Burning particles are ejected in the opposite direction of combustion by the heat flow and energy generated during the combustion process, creating a bright flame zone.

Microscale observations of the combustion process of the stick (Figs. 3(c) and 3(d)) revealed a wider chemical reaction zone for B-CuO, which is attributed to the greater heat of the explosion of B-CuO [13]. This causes a considerable part of the unreacted zone of the B-CuO stick to be heated up in advance due to heat propagation, and thus to enter the reaction zone in advance. The wide chemical reaction zone allows a large amount of B and CuO to react with each other per unit time, which has a positive effect on the combustion rate.

We recorded the combustion flame displacement of B-CuO, and B-Bi_2O_3 sticks at the same time intervals. The results show that the homogeneous mixing of boron and metal oxides can substantially improve the combustion stability of the stick, which is manifested in the burning rate as the displacement-time image of the combustion flame of the stick is a straight line slanting upward, and the presence of the broader chemistry makes the reaction rate of the B-CuO stick increase substantially up to 42.11 $mm \cdot s^{-1}$, which is about 2.3 times of the burning rate of the B-Bi_2O_3 stick (17.84 $mm \cdot s^{-1}$). We attribute this difference to the different heat release of the two wires. DSC tests on B-CuO and B-Bi_2O_3 sticks show that the heat release of B-CuO sticks (2377 $J \cdot g^{-1}$) is much larger than that of B-Bi_2O_3 sticks (526 $J \cdot g^{-1}$), and that the large amount of heat release gives the B-CuO sticks a much faster burning rate.

In addition, we found that the combustion reaction zone of the B-CuO stick pushes larger and brighter particles into the flame zone compared to the B-Bi_2O_3 stick, and hypothesized that this phenomenon is related to the melting points of Bi_2O_3 and CuO. It has been shown that partial sintering of metal oxides will take place at Taman temperatures, which will cause some movement of the metal oxides, and this movement will increase the contact area between the fuel and the oxidizer, making the reaction easier to carry out [27]. Because the melting point of Bi_2O_3 (825 ℃) is much lower than that of CuO (1446 ℃), it allows the B-Bi_2O_3 pharmacophore to react at relatively low temperatures. DSC also proved the existence of this phenomenon (Figs. 3(f) and 3(g)), with the B-Bi_2O_3 pharmacophore starting to react as early as 508 ℃ and peaking at 510 ℃, while the B-CuO pharmacophore reacted at 515 ℃ and peaked at 582 ℃.

In addition, Bi_2O_3 produces not only O_2 but also Bi gas during decomposition [1], and the vapor pressure of bismuth is higher than that of copper, which is conducive to the diffusion of bismuth vapors in the reactants and limits their premature condensation, thus achieving an increase in the effect and range of sparks [13]. In summary, the B-Bi_2O_3 stick reacts and produces more gas-phase material at lower temperatures during combustion. B-CuO, on the other hand, is a solid-solid phase reaction [28], and although the addition of F_{2602} causes the reaction to produce a small amount of BF_3 gas, the combustion process of the B-CuO stick is still a solid-solid phase that should dominate the reaction. The TG tests of B-CuO and B-Bi_2O_3 sticks (Figs. 3(f) and 3(g)) provide a favorable proof for this interpretation, and both B-CuO and B-Bi_2O_3 sticks have a mass reduction step before the reaction between the fuel and the oxide occurs. This is a reaction between F_{2602} and the initial oxide layer of boron, and after this step, B-CuO then undergoes a solid-solid phase reaction with no further change in mass, whereas B-Bi_2O_3 still suffers a substantial mass loss during the reaction. The microscale combustion image (Fig. 3(d)) illustrates this phenomenon. The reaction produces scorching particles that collide with each other and form larger granular combustion nodules, the B-CuO combustion process is the generation of trace gases and the stripping and ejection of large scorching burning particles.

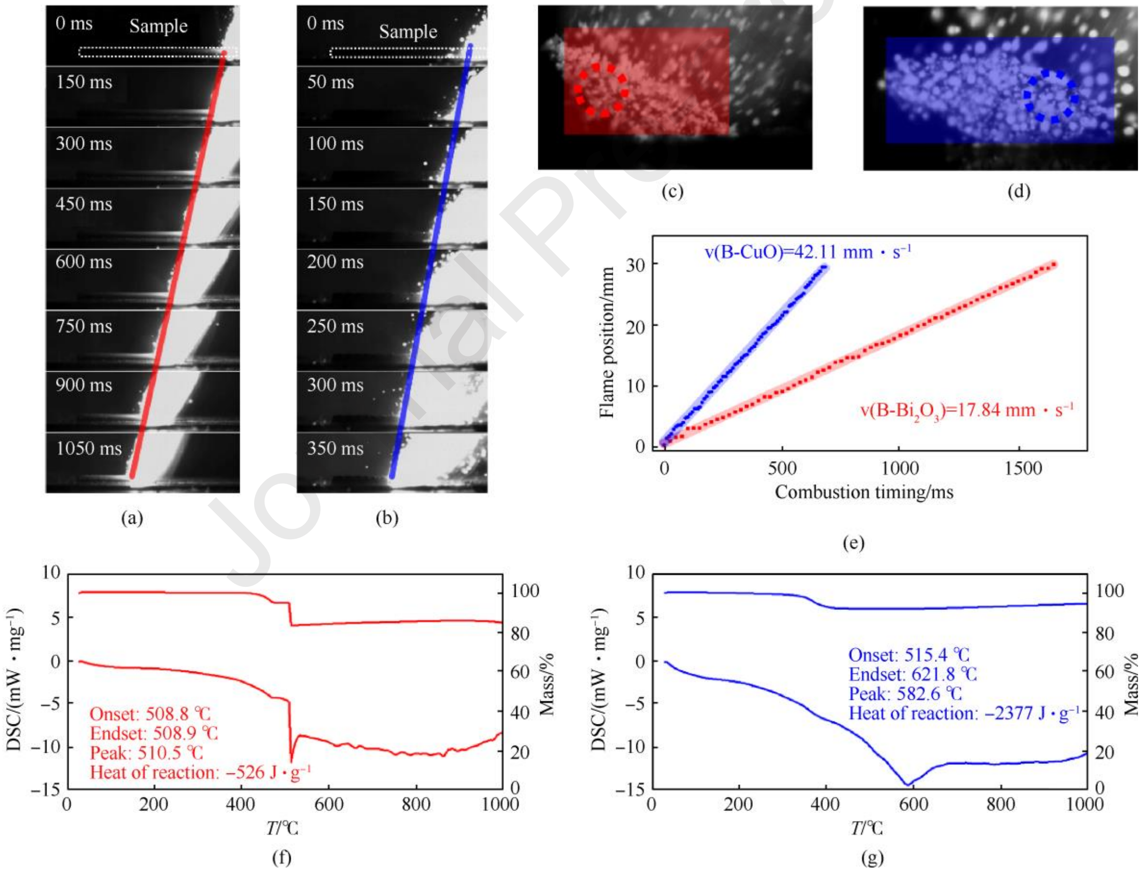

Fig. 3. (a), (c) Snapshots of the combustion and microscopic combustion map of B-Bi_2O_3 sticks; (b), (d) Snapshots of the combustion and microscopic combustion map of B-CuO sticks; (e) Flame displacement-time plots and fitting curve of combustion of B-CuO and Bi_2O_3 sticks; (f), (g) DSC-TG curves of B-CuO and B-Bi_2O_3 sticks.

3.3. Combustion properties of three-component micro-scale composite sticks

The combustion behavior of microscopic scale compounding of sticks was explored by compounding three-component inks in different ratios (B-CuO: B-Bi_2O_3=2:1; 1:1; 1:2) at the microscopic level.

Characterizing the combustion behavior and burning rate of the sticks, we found that sample 3#

with the highest CuO content (58.7%) has the highest reaction performance, and the large amount of CuO in the sample enhances the energy released from the combustion of the sticks, which can be used to pre-heat the un-reacted zone. The burning rate of sample 3# was as high as 60.59 mm·s^{-1}, much higher than that of the two-component B-CuO stick (42.11 mm·s^{-1}). The addition of B-Bi_2O_3 allows for a higher rate of energy release from the composite stick, a phenomenon we attribute to the lower melting temperature of Bi_2O_3, which allows it to move slowly at Taman temperatures, resulting in a reaction that can take place earlier, and a large amount of heat released from the B-CuO reaction allows the stick to burn more efficiently. With the increase of the Bi_2O_3 component in the stick, the burning rate of the stick first plummets, and then slowly rises in the burning rate of Bi_2O_3 stick component B-CuO two-component stick, which explains the combustion-promoting effect of B-Bi_2O_3 on the B-CuO component is limited. The amount of exothermic combustion of the components of the stick directly affects the combustion rate of the stick, with the reduction of the B-CuO component of the stick, the stick combustion heat is a downward trend, resulting in the intensity of the reaction of the stick, the width of the reaction zone has decreased, the stick combustion rate has also had a significant decline. It is worth noting that although the stick burning rate decreases significantly, its burning rate level is still much higher than the B-Bi_2O_3 stick burning rate.

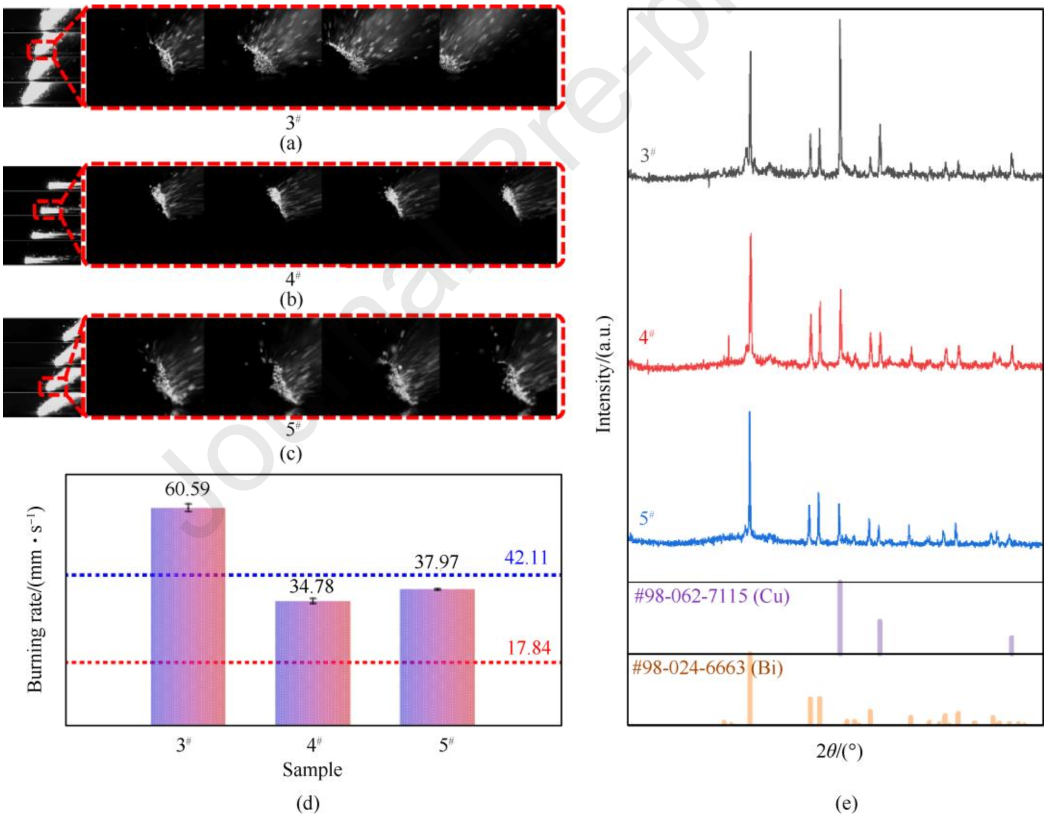

Fig. 4. Combustion diagrams of micro-scale composite sticks (a) 3#; (b) 4#; (c) 5#; (d) Combustion velocity maps of the sticks; (e) XRD of the combustion products of the sticks.

Analysis of the combustion product crystal shape of the stick can be seen, in the microscopic mixed state of the stick despite the presence of Bi_2O_3 and CuO, but the combustion process does not have two oxidant material exchange, the combustion process can be approximated as an independent redox reaction of B-CuO and B-Bi_2O_3, and combustion products for the crystals of Cu, Bi (Fig. 4(e)).

3.4. Combustion properties of three-component macro-scale composite sticks

We obtained three kinds of B-Bi_2O_3/B-CuO composite sticks with different accumulation modes with the help of double nozzle direct ink writing device (by the difference of their accumulation modes, the three kinds of sticks were abbreviated as BCBC, BBCC and 5B5C) by taking B-Bi_2O_3 and B-CuO inks with an equivalence ratio of 1.5 as the components, and the combustion performance test was carried out on them.

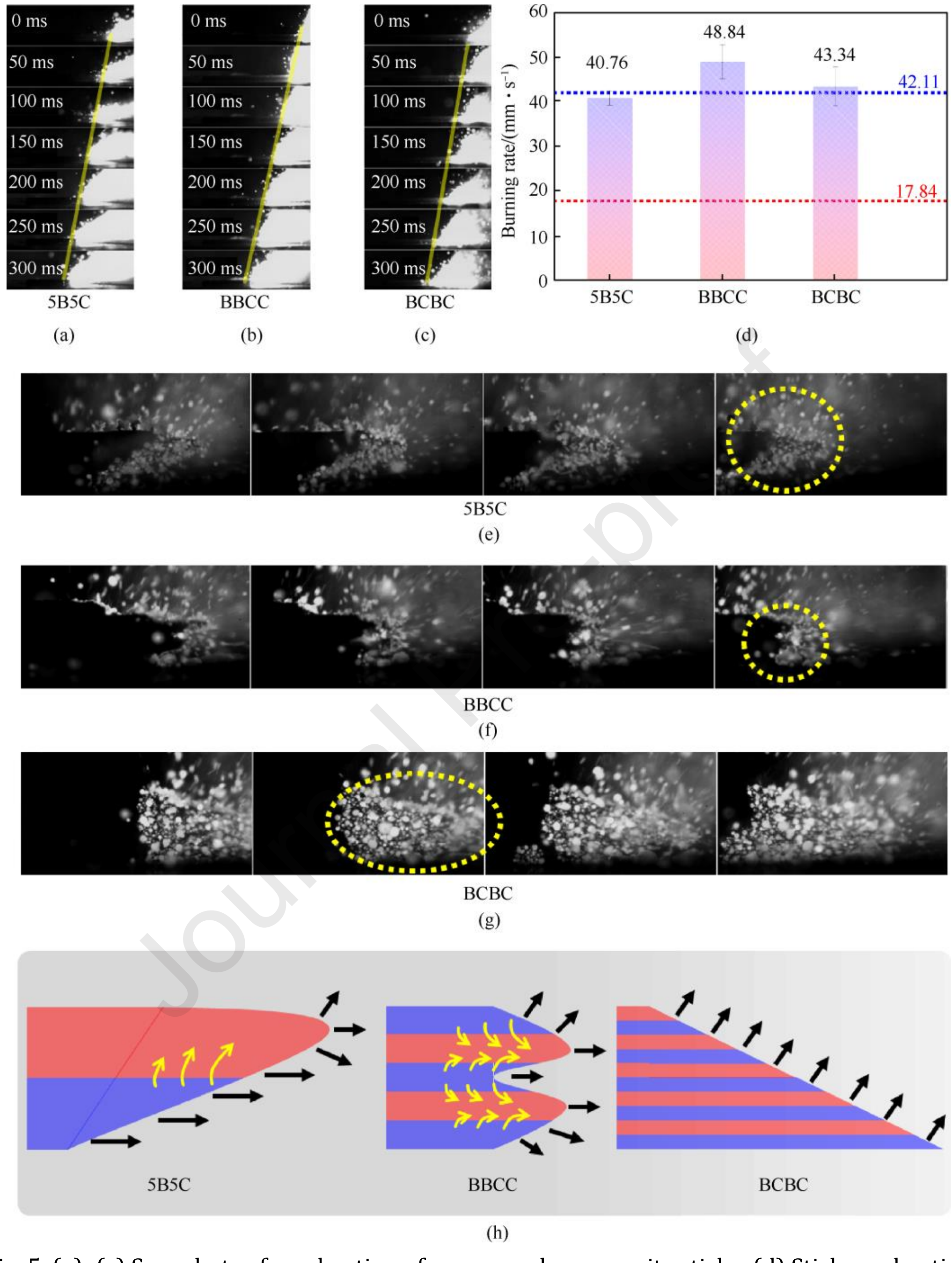

Fig. 5. (a)–(c) Snapshots of combustion of macro-scale composite sticks; (d) Stick combustion velocity map; (e)–(g) Microscopic combustion map of the stick; (h) Schematic diagram of the combustion process of the stick.

The test results are shown in Fig. 5. The combustion process of the sticks obtained by the three different accumulation methods was stable and the flames were relatively homogeneous (Figs. 5(a)–5(c)).

The burning velocities obtained by *X*-direction tracking of the combustion flame of each stick showed that macro-scale compounding increased the burning rate of the B-Bi_2O_3 component in the stick by about 150%, making the stick burning rate converge to that of CuO (42.11 mm·s^{-1}), and it is hypothesized that the heat released from the combustion of B-CuO and the material exchange between the two components generated during the combustion process have a certain thermal effect on the vitrification produced during the combustion process of B-Bi_2O_3, which makes the Bi_2O_3 to contact and react with boron nuclei more efficiently.

Differences in the degree of homogeneity of the three-component composite of B-Bi_2O_3 and B-CuO show very different combustion patterns (Figs. 5(e)–5(h)): When the stick is 5 layers of B-CuO and 5 layers of B-Bi_2O_3 phase composite (5B5C), the burning rate is the slowest (40.76 mm·s^{-1}), at this time, there is a phenomenon of divisional combustion in the stick, the lower layer of the faster combustion rate of the faster burning speed of B-CuO. This makes the B-CuO combustion peak ahead of the B-Bi_2O_3 part, and the heat released from the B-CuO combustion acts on the unreacted area of the B-Bi_2O_3 part, making the unreacted B and Bi_2O_3 heated up ahead of time, which will greatly enhance the reaction rate of the B-Bi_2O_3 part. With the further uniform composite (BBCC) of the three-component of the stick, the partition combustion phenomenon of the stick is more obvious, The combustion of the drug line is divided into three faster B-CuO combustion surfaces and the interphase in which the B-Bi_2O_3 combustion surface, compared with the composite of the 5B5C, the B-CuO combustion surface is still in the lead, the more tightly composite makes the combustion of the B-CuO portion of the heat transfer is more centralized, the heat transfer is more, which is manifested as a reduction in the distance between the two combustion surfaces. When the stick is in the densest buildup at the macroscopic level (BCBC), the bicomponent in the stick is further compounded, at which time the fractional combustion phenomenon of the stick is difficult to observe and is replaced by a homogeneous and inclined combustion surface, and the width of the combustion reaction zone of the stick is surged, similar to that of the reaction zone of the B-CuO, and the stick burning rate is 43.34 mm·s^{-1}, which is closer to that of the B-CuO (42.11 mm·s^{-1}).

It is worth noting that the composite mode of BBCC has a higher reactivity and the fastest burning rate (48.84 mm·s^{-1}) compared with BCBC, which is caused by the fact that the B-CuO portion of the BBCC stick is more, which accounts for 60% of the total volume, higher than that of the BCBC (50%), and a large amount of B-CuO will release more heat during the combustion of the stick, while some of the gases generated during the combustion of the B-Bi_2O_3 stick can blow the burning particles to the unreacted area, where the burning particles start to react quickly. A large amount of B-CuO will cause the stick to release more heat during the combustion process, and part of the gas generated during the combustion process of the B-Bi_2O_3 stick can blow the burning particles to the unreacted area, which will start the rapid reaction at the contact between the burning particles and the stick, thus enhancing the reactivity of the stick, and thus increasing the combustion rate.

In the crystallographic tests of the combustion products (Fig. 6(a)), we found that: when the sticks were composited at the macroscopic scale, BiF_3 appeared in the combustion products, which was not observed in the microscopic scale composites, and we attribute this to the fact that: in the macroscopic scale composites of the sticks, the phenomenon of partial combustion causes the F-containing gases produced by the B-CuO portion to be blown into the unreacted zone of the B-Bi_2O_3 portion, which will increase the F content within the reactive zone of the Bi_2O_3 fraction, which results in the presence of not only oxidized B_2O_3, reduced Cu and Bi, but also fluorinated BiF_3 in the combustion products (Fig. 6(a)). The EDS in the combustion products (Figs. 6(b)–6(d)) also lead to the corresponding conclusions that the elemental highlight regions of Bi and F are one-to-one, and the elements of B and O also have a high degree of overlap in their distributions because the boron feedstock that we used is amorphous, so its oxidation products cannot be reflected in the XRD. In addition, when the three components in the stick are more dispersed (5B5C, BBCC), the stick combustion performance is approximated as the separate combustion of B-CuO and B-Bi_2O_3, and there is a very small amount of material exchange during the combustion process, and the combustion products have obvious Cu and Bi zones (Figs. 6(b)–6(d)). When the stick macroscopic composite behaves as the densest composite (BCBC), the stick combustion behaves as a two-component co-combustion, and the molten Bi_2O_3 moves to the vicinity of CuO and reacts with B to sinter into large-scale particles of Cu, Bi, and B_2O_3.

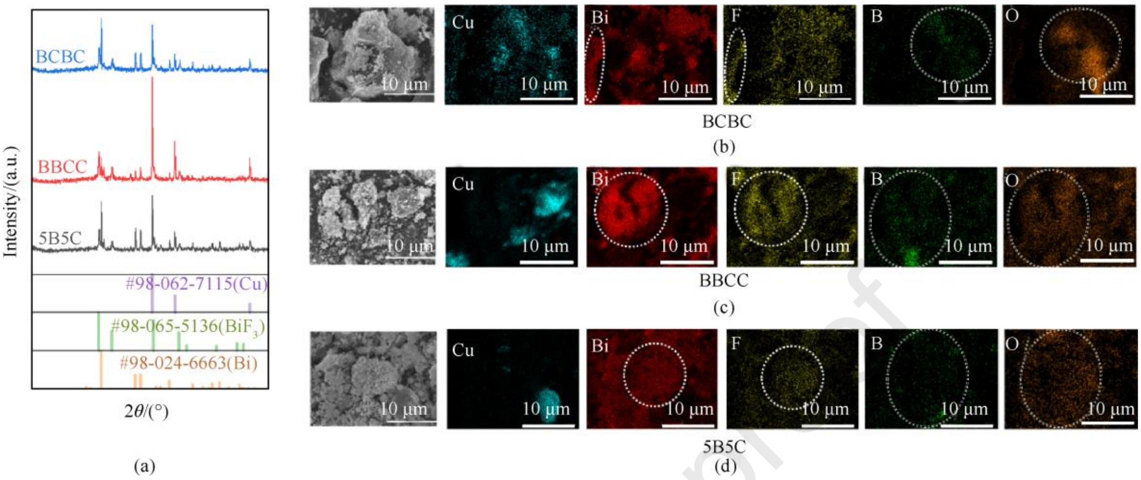

Fig. 6. (a) XRD test plots of the combustion products of macro-scale composite sticks; (b)–(d) EDS plots of the combustion products of macro-scale composite sticks.

In summary, we attribute the increase in the combustion rate of the B-Bi_2O_3 portion of the stick to the fact that a large amount of heat generated in the B-CuO portion of the stick is transferred to the unreacted zone of B-Bi_2O_3, which pre-activates the stick and greatly shortens the reaction course, thus enhancing the reaction rate of the stick. In addition, the macroscopic scale composite stick is more conducive to Bi fluorination due to the presence of B-CuO over-combustion, which makes the F-containing gas generated by combustion flow into the unreacted area of B-Bi_2O_3, and raises the F content in the reacted area of the B-Bi_2O_3 portion, which is beneficial for Bi fluorination, which has a certain effect on the enhancement of the burning rate of the stick.

4. Conclusions

In this study, B, CuO, and Bi_2O_3 were loaded into the dispersed phase DMF using F_{2602} as a binder, and the corresponding inks were obtained, and sticks composited with different contents of B-CuO and B-Bi_2O_3 at micro and macro scales were prepared with the help of the double nozzle direct ink writing device.

The combustion properties of two-component B-CuO and B-Bi_2O_3 sticks were investigated, and the B-CuO stick achieved the fastest burning rate (42.11 mm·s^{-1}) due to its higher exothermic heat of combustion, whereas Bi_2O_3 had a lower reaction rate (17.84 mm·s^{-1}) due to its lower reaction temperature and the glassy medium produced during combustion. On this basis, we tested the combustion performance of the B-CuO and B-Bi_2O_3 macro- and micro-scale composite sticks. In the macro-composite sticks, we found a combustion stratification phenomenon, the B-CuO portion with a faster burning rate transfers the heat and the combustion products to the un-reacted B-Bi_2O_3 portion, which then enhances the combustion rate of the B-Bi_2O_3 portion. The burning rate of the B-Bi_2O_3 part was enhanced. In summary, the multiscale molding of B, CuO, and Bi_2O_3 was carried out by a double nozzle direct ink writing device, and the energy release behaviors of macroscopic and microscopic scale composite flux lines were discussed, which provided a new idea and a new method for the composite of multivariate powders.

References

[1] Jian G, Chowdhury S, Sullivan K, Zachariah MR. Nanothermite reactions: Is gas phase o xygen generation from the oxygen carrier an essential prerequisite to ignition? Combust Flame 2013;160:432–7. https://doi.org/10.1016/j.combustflame.2012.09.009.

[2] Abraham A, Piekiel NW, Morris CJ, Dreizin EL. Combustion of Energetic Porous Silicon Composites Containing Different Oxidizers. PROPELLANTS Explos Pyrotech 2016;41:179–88. https://doi.org/10.1002/prep.201500108.

[3] Luo, Q-P. Study on the Reaction Properties of Al/Fe2O3-RDX Nanocomposites. Beijing In stitute of Technology, 2015.

[4] Thakur P, Sharma V, Thakur N. Study of energy release in Fe2O3/Al nano-thermite wit h graphene as an additional fuel. Phys B-Condens MATTER 2021;610:412803. https://d oi.org/10.1016/j.physb.2020.412803.

[5] Wang LL, Munir ZA, Maximov YM. Thermite reactions: their utilization in the synthesis and processing of materials. J Mater Sci 1993;28:3693–708.

[6] Alvarez F, Delgado A, Frias J, Rubio M, White C, Swamy AKN, et al. Microgravity combu stion of thermite mixtures for welding in space and for production of structural materi als from lunar regolith. 50th AIAA Aerosp. Sci. Meet. New Horiz. Forum Aerosp. Expo. J anuary 9 2012 - January 12 2012, Nashville, TN, United States: AIAA International; 201 2. https://doi.org/10.2514/6.2012-1119.

[7] Wang S, Xin W, Qu L, Wu Y, Yang J. Study on length of cartridge how to affects cuttin g capability of the combustion cutting ammunition. 2012 Int. Conf. Appl. Mech. Mater. I CAMM 2012 Novemb. 24 2012 - Novemb. 25 2012, vol. 275–277, Sanya, China: Trans Tech Publications; 2013, p. 2248–51. https://doi.org/10.4028/www.scientific.net/AMM.27 5-277.2248.

[8] Fahd A, Baranovsky A, Dubois C, Chaouki J, Wen JZ. Superior performance of quaternar y NC/GO/Al/KClO4 nanothermite for high speed impulse small-scale propulsion applicati ons. Combust FLAME 2021;232:111527. https://doi.org/10.1016/j.combustflame.2021.111 527.

[9] Pang W-Q, Yetter RA, DeLuca LT, Zarko V, Gany A, Zhang X-H. Boron-based composite e nergetic materials (B-CEMs): Preparation, combustion and applications. Prog ENERGY Co mbust Sci 2022;93:101038. https://doi.org/10.1016/j.pecs.2022.101038.

[10] Han L, Wang R, Chen W, Wang Z, Zhu X, Huang T. Preparation and Combustion Mecha nism of Boron-Based High-Energy Fuels. CATALYSTS 2023;13:378. https://doi.org/10.339 0/catal13020378.

[11] Liu T, Chen X, Han AJ, Ye MQ, Zhang ST. Preparation and Properties of Boron-Based Na no-B/CuO Thermite. KnE Mater Sci 2016. https://doi.org/10.18502/KMS.V1I1.569.

[12] Liu T, Chen X, Xu H, Han A, Ye M, Pan G. Preparation and Properties of Boron-Based Nano-B/NiO Thermite. PROPELLANTS Explos Pyrotech 2015;40:873–9. https://doi.org/10. 1002/prep.201400308.

[13] Comet M, Schnell F, Pichot V, Mory J, Risse B, Spitzer D. Boron as fuel for ceramic the rmites. Energy Fuels 2014;28:4139–48. https://doi.org/10.1021/ef500221p.

[14] Gottfried JL, Wainwright ER, Huang S, Jiang Y, Zheng X. Probing boron thermite energy release at rapid heating rates. Combust FLAME 2021;231:111491. https://doi.org/10.101 6/j.combustflame.2021.111491.

[15] Valluri SK, Gandhi PM, Schoenitz M, Dreizin EL. Boron-Rich Composite Thermite Powde

rs with Binary Bi_2O_3 center dot CuO Oxidizers. ENERGY FUELS 2021;35:10327–38. https://doi.org/10.1021/acs.energyfuels.1c01052.

[16] Cao, Y. Study on Laser-MicroPen/MicroJet Direct WritingTechnology for Integrated Fabrication of MEMS Micro Structures. Huazhong University of Science & Technology,2009.

[17] Peng, CZ. Additive Manufacturing for Energetic Materials: Emerging Precision Loading & Efficient and Safe Preparation Technology. Chinese Journal of Energetic Materials 2019;27;445–7.

[18] Li, CY; Wen, K;An, CW; Song, HY; Ye, BY; Wu, BD; Wang, JY. Effect of Binder on Formability and Combustion Performance of B/KNO3 Samples by Direct Ink Writing. Chinese Journal of Energetic Materials 2022;30;332–40.

[19] Li C, Song H, Xu C, Li C, Jing J, Ye B, et al. Reactivity regulation of B/KNO3/PVDF energetic sticks prepared by direct ink writing. Chem Eng J 2022;450:138376. https://doi.org/10.1016/j.cej.2022.138376.

[20] Song, HY; Li, CY; An, CW; Wang, JY. Study on Combustion and Delay Performance of B/CuO Delay Compositions. Chinese Journal of Explosives & Propellants 2022;45;722–9. https://doi.org/10.14077/j.issn.1007-7812.202204002.

[21] Ruz-Nuglo FD, Groven LJ. 3-D Printing and Development of Fluoropolymer Based Reactive Inks. Adv Eng Mater 2018;20:1700390. https://doi.org/10.1002/adem.201700390.

[22] Shen J, Wang H, Kline DJ, Yang Y, Wang X, Rehwoldt M, et al. Combustion of 3D printed 90 wt% loading reinforced nanothermite. Combust Flame 2020;215:86–92. https://doi.org/10.1016/j.combustflame.2020.01.021.

[23] Li Q, An C, Han X, Xu C, Song C, Ye B, et al. CL-20 based Explosive Ink of Emulsion Binder System for Direct Ink Writing. PROPELLANTS Explos Pyrotech 2018;43:533–7. https://doi.org/10.1002/prep.201800064.

[24] Xie Z, An C, Ye B, Mu J, Li C, Li M, et al. 3D direct writing and micro detonation of CL-20 based explosive ink containing O/W emulsion binder. Def Technol 2022;18:1340–8. https://doi.org/10.1016/j.dt.2021.09.0072214-9147.

[25] Zhong L, Mao Y, Zhou X, Zheng D, Guo C, Wang R, et al. 3D printing of hollow fiber nanothermites with cavity-mediated self-accelerating combustion. J Appl Phys 2021;129:105105. https://doi.org/10.1063/5.0039604.

[26] Zhou X, Mao Y, Zheng D, Zhong L, Wang R, Gao B, et al. 3D printing of RDX-based aluminized high explosives with gradient structure, significantly altering the critical dimensions. J Mater Sci 2021;56:9171–82. https://doi.org/10.1007/s10853-021-05869-3.

[27] Wu T. Exploring the Relationships Between Fuel and Oxidizer Reaction of Biocidal Energetic Materials. Ph.D. University of Maryland, College Park, 2019.

[28] Li, YC; Hui, YL; C, Y. Study on Thermokinetics Analysis of B/CuO Delay Composition. Initiators & Pyrotechnics **2009**;22–24.

we have no known competing financial interests or personal relationships that could have appeared to influence the work reported in this paper.